Composites Part B 101 (2016) 87–98

Contents lists available at ScienceDirect

Composites Part B

journal homepage: www.elsevier.com/locate/compositesb

Influence of B_4C particle reinforcement on mechanical and machining properties of Al6061/B_4C composites

Şener Karabulut [a,*], Halil Karakoç [a], Ramazan Çıtak [b]

[a] Department of Mechanical Program, Hacettepe University, 06935 Ankara, Turkey
[b] Department of Metallurgy and Materials Eng., Gazi University, 06500 Ankara, Turkey

ARTICLE INFO

Article history:
Received 26 April 2016
Received in revised form
3 June 2016
Accepted 5 July 2016
Available online 6 July 2016

Keywords:
Metal-matrix composites (MMCs)
Mechanical properties
Surface properties
Machining
Milling

ABSTRACT

This study investigates the mechanical and machinability properties of the aluminum 6061 reinforced with boron carbide (B_4C). Four aluminum 6061 composite specimens reinforced with 5 wt%, 10 wt%, 15 wt%, and 20 wt% B_4C were fabricated using a powder metallurgy and hot-extrusion method. The composite samples were investigated to elucidate the influence of different weight fractions of B_4C reinforcement content on the hardness, fracture toughness, tensile strength, transverse rupture strength (TRS) and milling properties of the resulting composites. The milling tests were performed based on the Taguchi mixed-orthogonal-array for experiments, L_{16} ($4^4 \times 2^1$), to determine the effect of B_4C content on surface quality and energy consumption for different cutting parameters under dry- and compressed-air cooling and using an uncoated carbide insert. The results reveal that the B_4C particles are uniformly distributed in the matrix and that the fracture toughness decreases and the hardness increases as the weight fraction of the reinforcement increases. The highest tensile and transverse rupture strength are for Al6061/5 wt% B_4C and Al6061 reinforced with 10 wt% B_4C composite material has the best fracture toughness from among the specimens measured. At higher milling speed and lower cutting feed and under dry machining conditions, an excellent surface quality is obtained after milling all composites materials and the surface finish improves with increasing B_4C content in the matrix. The power consumption and surface roughness increases when cooling with compressed air.

1. Introduction

Boron carbide (B_4C) is an extremely hard reinforcement material with excellent hardness, corrosion resistance, and mechanical properties, which makes it a desirable material for a number of engineering applications. B_4C has excellent ballistic characteristics due to its high hardness, low density, high melting point, and thermal stability, and it is widely used in refractory applications requiring high-resistance materials, such as ballistic protection, for tank armor, and in the nuclear-power industry as a neutron-radiation absorber [1,2]. Aluminum and aluminum-based metal matrix composites (MMCs) have become attractive engineering materials in several applications, such as armor, the nuclear-power industry, and for aerospace, automotive, marine, and automobile products because of their low density and superior mechanical properties such as hardness, wear resistance, and tensile and flexural strengths. At the same time, the machinability of metal matrix composites is difficult because of the hard reinforcement particles in the aluminum matrix [3–7]. Rajkumar et al. [8] produced aluminum-B_4C (Al-B_4C) 5%–15% composites using a stir-casting method. They investigated the mechanical and machinability characteristics in a turning machine. The impact decreases and the hardness increases with the reinforcement content. The cutting force decreases at higher machining speed and increases at greater cutting depth during the milling of composites. Ibrahim et al. [9] three aluminum 6063 based metal matrix composites reinforced with 15 vol% B_4C were fabricated using the molten metal processing method. The B_4C particles were injected into molten aluminum using a powder injection technique and compositions were homogenized to obtain a uniform microstructure at the elevated temperatures for 48 h. Then, resulting specimens were quenched in warm water and aged in the range of 25–400 °C for 10 h, at each temperature. They were also investigated the heat treatment conditions on the hardness, tensile and fracture behavior on three MMCs reinforced with 15 vol% B_4C. The authors obtained a homogenous particle distribution and strong interfacial bonding

* Corresponding author.
E-mail address: senerkarabulut@hacettepe.edu.tr (Karabulut).

http://dx.doi.org/10.1016/j.compositesb.2016.07.006
1359-8368/

with the aluminum matrix. The mechanical behavior of the resulting composites was improved after an aging process. In another study, Ibrahim et al. [10] investigated the impact toughness of Al–15 vol% B_4C MMCs. Experimental samples were produced and prepared as described in the previous study mixing small amount of Ti, Zr and Sc. The presence of Ti was enhanced the wettability of B_4C particles and their bonding in the matrix structure. Al-based MMCs showed better toughness and the composite impact toughness was affected by the precipitation phases. Baradeswaran and Perumal investigated the effect of B_4C on the mechanical and tribological mechanical properties of Al 7075–B_4C composites [11]. The experimental results showed that the hardness, ultimate tensile, compression, flexural strength and wear resistance of the composites improved with increasing content of B_4C particles. Karabulut et al. produced the three composites reinforced with 10 wt% Al_2O_3, 10 wt% B_4C, and 10 wt% SiC using a powder metallurgy and hot-extrusion method. They investigated the hardness, transverse rupture strength, elongation and drilling properties of these composites. The highest mechanical results and better hole surface quality were obtained in AA7039 composite reinforced with 10 wt% Al_2O_3 [12]. Joshua et al. [13] studied how cutting parameters affect surface quality when end milling Al6061 and derived an equation to predict surface roughness. They performed 120 milling experiments under dry and minimum-quantity-lubrication (MQL) environments using high-speed-steel cutting tools. They observed that cutting feed is most effective for controlling surface integrity and that the best surface roughness occurs under MQL cutting conditions. Lou et al. [14] developed a model to predict surface roughness for milling Al6061. They found that cutting feed is the most significant milling parameter for surface roughness. Lillo [15] investigated the ductility properties of Al6061 by reinforcing 10 wt% B_4C using equal-channel angular extrusion processing (ECAP). The author reported that the tensile strength of MMCs is improved by using the ECAP method. Chen et al. [16] studied the mechanical behavior of Al6061 and of Al6061 reinforced with an Al_2O_3 composite after ECAP. The measurements show that, compared with unreinforced Al6061, the tensile and fatigue strengths of Al6061/Al_2O_3 composite are significantly enhanced after ECAP. Rao et al. [17] investigated the aging of ultrafine-grained Al6061 alloy by using multidirectional forging at cryogenic temperatures. The results show that a homogeneous microstructure develops, and the tensile strength of the material improves significantly upon aging. Camposeco [18] investigated the optimal turning parameters for roughing machining of AISI 6061 T6 aluminum. He states that the depth of cut and cutting feed are the most significant factors for minimizing energy consumption and surface roughness. Patel et al. [19] studied how various machining factors affect surface quality and energy consumption in the turning of Al6063 alloy TiC composite. The experiment result indicates that feed rate is an effective parameter to control surface roughness and that cutting speed is a significant factor determining power consumption. Muñoz-Escalona et al. [20] studied the effect of machining environment on surface quality and energy consumption in the milling of austenitic stainless steel. The results indicate that the optimal power consumption and surface roughness occurs under dry-cutting conditions.

Aluminum 6061, which has the highest ductility and strength of the aluminum alloys with perfect machinability and good wear properties, is used as the matrix material [21]. Al6061 is typically used as a base matrix metal for MMCs reinforced with various particles and whiskers because of its corrosion resistance, castability, fluidity, and strength [22]. Based on a literature review, the effect on surface roughness and energy consumption of reinforcement with various amounts of B_4C, which affects the mechanical properties of the Al6061 matrix, has not been much investigated for milling Al6061 reinforced with B_4C when cutting under dry– and compressed–air cooling. In light of this and because of its increasing engineering use, the machining and mechanical properties of these composite materials need to be investigated in detail to allow rapid industrial use of these materials. Therefore, the objective of the present study is to investigate the influence of the various weight fractions of B_4C on the mechanical characteristics and machining behavior of Al 6061 – B_4C composites. For this purpose, Al-B_4C (Al6061–B_4C; 5%–20%) composites were produced using the powder metallurgy method and their mechanical properties were analyzed. Subsequently, milling experiments were conducted to better understand the machinability of these composite materials and the machining parameters that determine surface quality and power consumption. The quality of the finished surface is one of the most significant demand to the improvement in productivity and the reduction of production cost for intensive milling operations, along with the mechanical properties of the workpiece such as abrasion, creep, fatigue strength, and corrosion resistance. Machining parameters and cutting environment are also very important factors to consider for producing a high quality-machined surface with minimal cost. If the cutting conditions are not determined properly, the machining process may result in the error of the machine limitations and workpiece quality, or reduced productivity. Thus, we studied how the weight fraction of B_4C particles affect surface roughness, productivity and power consumption when using uncoated carbide insert, for various milling parameters, and under dry- and compressed-air cooling. Finally, the composite materials are compared based on their mechanical properties, surface roughness, and energy consumption to specify the machining parameters for producing new composite materials. Furthermore, analysis of variance (ANOVA) was used to evaluate the experimental results and the optimal machining parameters were specified.

2. Experiment procedure

2.1. Workpiece material

The experimental workpieces were produced from high-purity Al6061 reinforced with 5 wt%, 10 wt%, 15 wt%, and 20 wt% commercial-grade B_4C powder using the powder metallurgy method. The chemical composition of Al6061 is given in Table 1. The median size of Al6061 powder used in the MMC was 100 μm and the B_4C powder had an average size of 10 μm. To achieve homogeneity, aluminum alloy and different weight fractions of B_4C powder were mixed separately and uniformly for 45 min in a three-dimensional Turbula mixer. The mixed Al6061/B_4C powder was compacted at 300 MPa. The cold-pressed specimens were sintered in a vacuum furnace at 550 °C for 60 min and then extruded using a preheated extrusion mold at 500 °C for 1 h. The dimensions of the composite sheets thus produced were 285 × 86 × 24 mm^3. The Al6061/B_4C composite materials were subjected to solution heat treatment at 530 °C for 1 h. To maximize the dissolution of Al6061, the solution heat treatment was performed as close as possible to the melting temperature. Next, specimens were hardened in water at room temperature. After solution treatment and quenching, composites were aged at 175 °C for 8 h in a furnace. The resulting specimens were subjected to hot rolling process to obtain 22 mm uniform thickness.

Table 1
Chemical composition of Al6061 aluminum alloy.

%Fe	%Si	%Cr	%Mn	%Mg	%Zn	%Cu	%Ti	%Al
0.5	0.6–1.0	0.1	0.2–0.8	0.8–1.2	0.25	0.6–1.1	0.1	Bal.

2.2. Analysis of microstructure and mechanical properties

Workpiece materials were analyzed using a JEOL JSM 6060 LW scanning electron microscope (SEM) and energy-dispersive spectroscopy (EDS). The machined surface of the specimens was polished and etched with a solution of 1 ml HF + 200 ml H_2O for 15 s; then, the microstructure of the composite samples was analyzed using a Leica DM4000 M microscope. The specimen hardness was measured using a hardness instrument (EMCO TEST Duravision 200) and applying a load of 31.25 kg for 5 s. The average hardness of each sample was determined by taking the average of the hardness measurements in five different areas. The impact energy of the composite samples was determined using a Charpy impact-measurement machine (Instron Wolpert PW30) with a maximum hammer energy of 150 J. Impact measurements were performed on V-notched specimens to determine the fracture toughness of the composite samples according to EN ISO 148.01. Tensile strength and TRS were measured using an Instron 3369 universal testing machine at a constant strain rate of 1 mm/s according to MPFI–10 [23] and MPFI–41 [24], respectively. Every impact, tensile, and TRS measurement was conducted at least three times and the average value of the three measurements was retained for the composites samples. Five mechanical test samples for each composite material were prepared using wire electrical discharge machining (WEDM) according to Metal Powder Industries Federation Standard Test Methods for Metal Powders and Powder Metallurgy Products (MPFI-41, 1998).

2.3. Machining process and milling parameters

The face-milling experiments were performed on a Doosan DNM 500 II Vertical Machining Centre with a maximum spindle speed of 8000 rpm and a maximum spindle motor power of 15 kW. The cutting speed, feed rate and axial depth of cut are the milling parameters of interest for this study, and the experiments were conducted under the machining environments of dry- and compressed-air cooling. The cutting parameters were determined based on previous research results, cutting-tool-manufacturer recommendations, and ISO Standard 8688-1 [25,26]. Selected milling variables and experimental levels are shown in Table 2. From the previous studies, it is concluded that poly crystalline diamond (PCD) tools were used in the machining of MMCs due to its superior hardness, fracture resistance, abrasion and thermal conductivity. On the other hand, PCD inserts are considerably costly in comparison with carbide inserts. Hence, carbide inserts have been determined advantageous in terms of machining costs with acceptable cutting tool wear in some cases in the literature [27] and preferred instead of PCDs in the milling experiments. A standard SK 40 tool holder with a single WK10-grade uncoated round positive cutting insert was used for the experiments. The cutting tool was produced by Walter, and it carries the ISO designation “RDGT 1204M0-G88 WK10.” It is recommended for milling aluminum alloy under various machining conditions. All experiment specimens were formed into 80 × 50 × 22 mm^3 blocks for face milling. The cutting length was 80 mm and all experimental trials were performed with two passes for all machining parameters. The energy consumption of the CNC machine tool was also recorded using a Fluke 43B series power-quality analyzer for each experiment involving active cutting. The chip conveyor turned off to reduce energy consumption during experiments, and for air cooling, compressed air was taken from an external compressed-air line by using a pneumatic polyurethane tube. Fig. 1 shows the experimental setup for milling, the specifications of the cutting insert, and the dimensions of the workpiece material.

2.4. Surface-roughness measurements

The surface of every specimens was machined with a new side of a cutting insert, and the surface-roughness measurements were made along the cutting direction of the finished surface using a Mitutoyo Surftest SJ-210 portable surface-roughness measurement instrument. The ISO 4287 standard [28] was followed for measuring the surface roughness. The surface roughness of each composite specimen was defined as the mean surface roughness measured at six points near the center of the machined samples and without removing the workpiece. The minimum and maximum results for surface roughness were rejected and the average surface roughness was computed using the four remaining values.

2.5. Experiment design and optimization

To investigate the effect of milling parameters on surface quality and energy consumption, experiments were conducted following Taguchi’s mixed-orthogonal-array design, L_{16} ($4^4 \times 2^1$). For this study, four different composite specimens were machined under two levels of dry- and compressed-air cooling. Three machining parameters—milling speed, feed rate, and axial cutting depth—were used as four-level milling parameters. Table 3 shows the Taguchi L_{16} mixed orthogonal array used to manage the experiments. The use of orthogonal arrays can decrease the time and cost of experiments by reducing the number of experiments. They also minimize the influence of factors that cannot be controlled. Furthermore, this approach provides an easy, effective, and systematic way to determine the ideal machining factors.

3. Experiment results and discussion

3.1. Microstructural and mechanical properties

Al6061-based MMCs reinforced with 5 wt% B_4C, 10 wt% B_4C, 15 wt% B_4C, and 20 wt% B_4C were fabricated using a powder

Table 2
Milling parameters for surface roughness and experiment levels.

Factors	Notation	Unit	Level 1	Level 2	Level 3	Level 4
A- Material	M		5 wt%B_4C	10 wt%B_4C	15 wt%B_4C	20 wt%B_4C
B- Milling speed	V_c	m/min	220	285	370	480
C- Feed rate	f_z	mm/tooth	0.08	0.1	0.12	0.16
D- Depth of cut	a_p	mm	0.8	1	1.3	1.7
E-Cutting environment	Ce		Dry	Compressed air		
Workpiece dimensions		mm		80 × 50 × 22		
Entering angle	K_r	Degree	90			
Cutting width	a_e	mm	22			
Cutting diameter	D_c	mm	40			
Number of tooth	z_n	*pcs*	1			

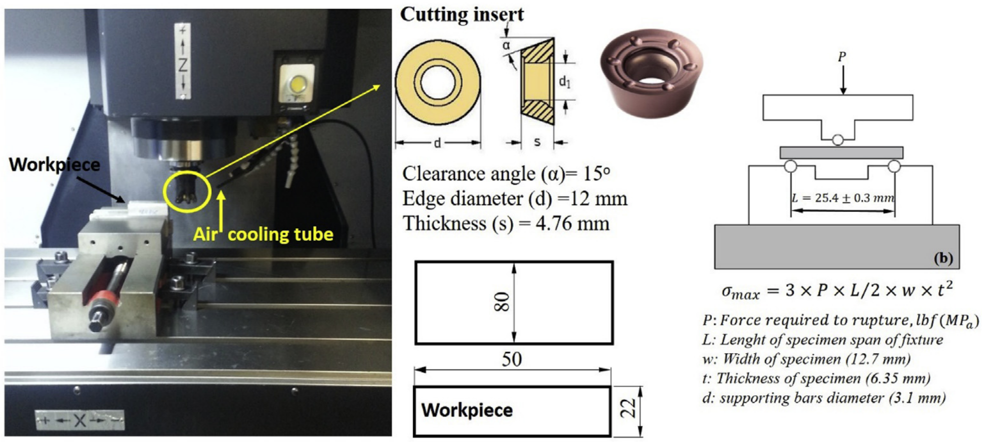

Fig. 1. Setup for milling and specifications of cutting insert (a), and the transverse rupture strength apparatus (b).

metallurgy method and hot-extrusion method. The specimens were subjected to solution heat treatment at 530 °C for 1 h to overcome the wettability problem between aluminum alloy and B4C and hardened in water at room temperature. Then, the resulting composites were aged at 175 °C for 8 h in a furnace and subjected to hot rolling process. The hardness, impact toughness, tensile and transverse rupture strength of the composites were investigated. Optical micrographs and SEM images of the surface texture of the machined composites and the distribution of B_4C particles are depicted in Figs. 2 and 3, respectively. As shown in these figures, B_4C particles were uniformly distributed in the matrix structure and some agglomerated particles were observed in 10 wt% B_4C specimen (Fig. 2). Better interface bonding was achieved between the matrix and B_4C particles. However, some interfacial voids were observed at one side of the B_4C particles and aluminum alloy interface due to the poor wetting properties of B_4C, as shown in Figs. 3 and 11.

The results of the hardness, fracture toughness, tensile and transverse rupture strength of the composite materials are presented in Fig. 4. The hardness of the composite samples increases with the increasing reinforcement volume of B_4C. The hardness of specimens was increased at the around of reinforcement particles in the matrix due to the improved strain energy. The maximum hardness is for Al6061 reinforced with 20 wt% B_4C. The highest tensile strength and TRS was measured of 5 wt% B_4C-reinforced composite specimens are better than those of the other composite materials studied. The TRS values were decreased with the increasing B_4C content and the tensile strength of specimens has exhibited an unstable behavior. The tensile strength of 5 wt%B_4C specimen first improved and then decreased with increasing the reinforcement B_4C particle. The tensile strength of 10 wt% B_4C-reinforced composite specimen is reduced from 210 MPa to 170 MPa and the tensile strength of 15 and 20 wt% B_4C-reinforced composites were significantly enhanced compared with the Al6061 alloy reinforced with 10 wt% B_4C. The improvement in the tensile strength of composites could be attributed to the transferring of load from aluminum matrix alloy to the hard reinforcement particles [29]. The lower tensile strength value for 10 wt% B_4C-reinforced composite specimen may be attributed to the agglomeration of reinforcement particles in the matrix structure (Fig. 2). The composite specimens were produced by using hot extrusion and then hot rolling method to achieve a uniform particles dispersion and strengthening the mechanism. Despite the using fabrication method, the voids exist at the matrix/particle interface indicating the weak interfacial bonding and the particles breakage was also observed at the machined surface of Al6061/10 wt% B_4C (Fig. 10). Hence, the decreasing tensile strength of Al6061/10 wt% B_4C may be a consequence of agglomeration and inadequate interface bond at the particles/matrix interface. The transverse rupture strength tests were performed to reveal the fracture behavior of the aluminum 6061 based composite specimens, with varying volume fraction of the B_4C particles. Fig. 5 depicts the influence of B_4C on the three-point bending strength of the composites. It is observed that the TRS was decreased from 562 MPa to 441 MPa on increasing the B_4C particles. The crack mechanism was seen at the bottom side of the all composite specimens at the end of the transverse rupture strength tests. However, no fractures were not occurred under study as shown in Fig. 5. These results indicated that the all composites reinforced with different weight fraction of B_4C had enough ductility to achieve more strength which caused an increase in the flexural strength from 562 MPa to 441 MPa. The fracture surface evaluation of the composites was performed on the Charpy impact testing specimens to clearly understand the crack initiation process. The highest fracture toughness is for Al6061/10% B_4C and decreases after this point, as expected based on the increasing fraction of the B_4C. Fracture surfaces of the composites are described by the presences of large deep voids and small dimples formed by B_4C particles indicating good ductility in Fig. 6. It was observed that B_4C particles were retained in the matrix after the fracture due to the good interfacial bonding effect in the matrix structure. The B_4C reinforcement particles were prevented the

Table 3
Taguchi L_{16} ($4^4 \times 2^1$) standard orthogonal array.

A	B	C	D	E
1	1	1	1	1
1	2	2	2	1
1	3	3	3	2
1	4	4	4	2
2	1	2	3	2
2	2	1	4	2
2	3	4	1	1
2	4	3	2	1
3	1	3	4	1
3	2	4	3	1
3	3	1	2	2
3	4	2	1	2
4	1	4	2	2
4	2	3	1	2
4	3	2	4	1
4	4	1	3	1

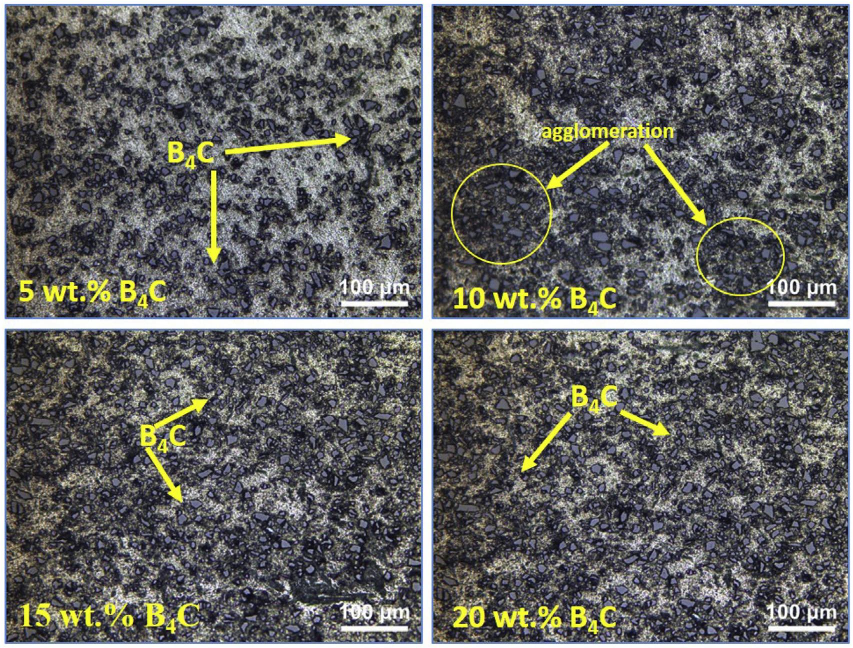

Fig. 2. Optical micrographs of composite materials under study.

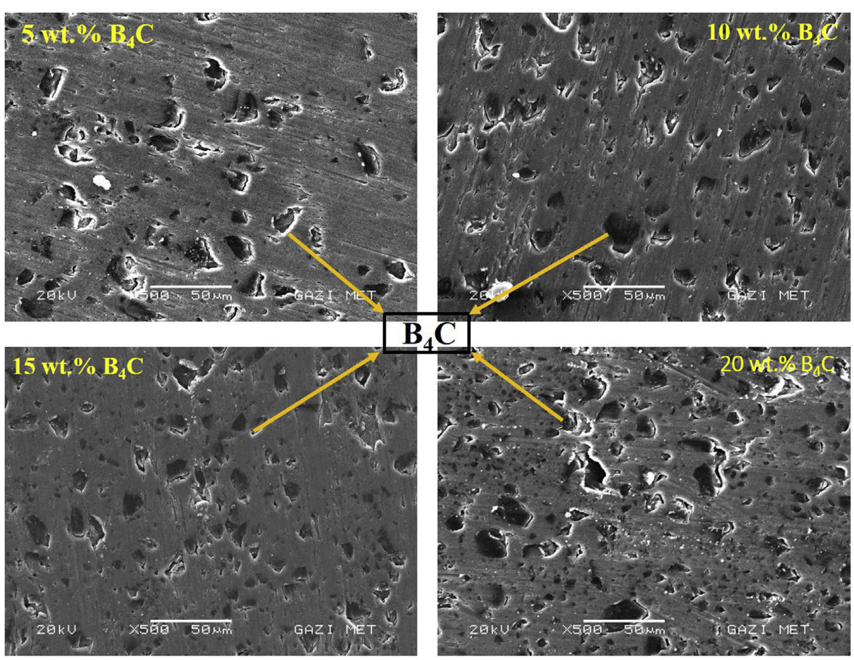

Fig. 3. SEM micrographs of machined workpiece materials.

quick progression of cracks through the matrix structure and limited the deformation of the composites, which enhanced the flexural strength of the composites. The B_4C particles intercepted the motion of dislocation and acted as crack stoppers.

3.2. Experimental design and optimization

Surface roughness and power consumption were measured by face-milling tests, and milling parameters were determined using the Taguchi techniques. A number of external parameters that are not considered in the design of the experiment affect the experimental results. These parameters and their effect on the result are categorized as "noise." The signal-to-noise ratio (S/N*)* is computed in two stages. First, the mean squared deviation (MSD) between the measured and target values are computed by using Eq. (1). Second, the MSDs are converted to S/N using Eq. (2) [30]. Next, the surface roughness and energy consumption are analyzed based on the S/N. The-smaller-the-better approach is used to determine the smallest surface roughness (*Ra*) and power consumption (*P*) based on the optimal milling parameters.

The following equations are used to compute the S/N ratios:

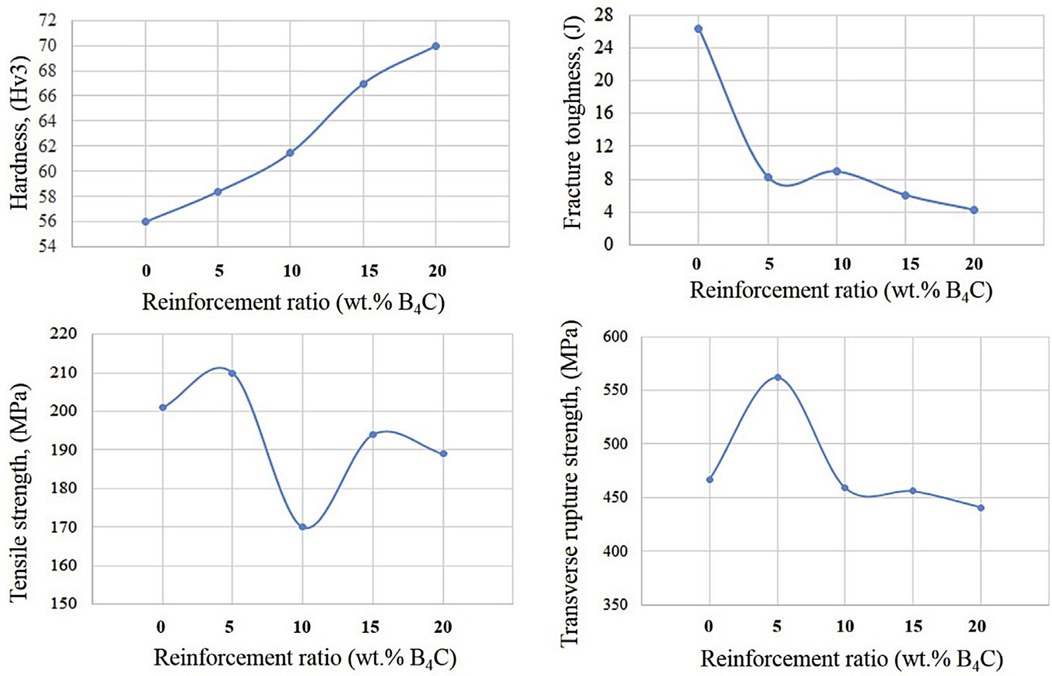

Fig. 4. Mechanical properties of composite materials under study.

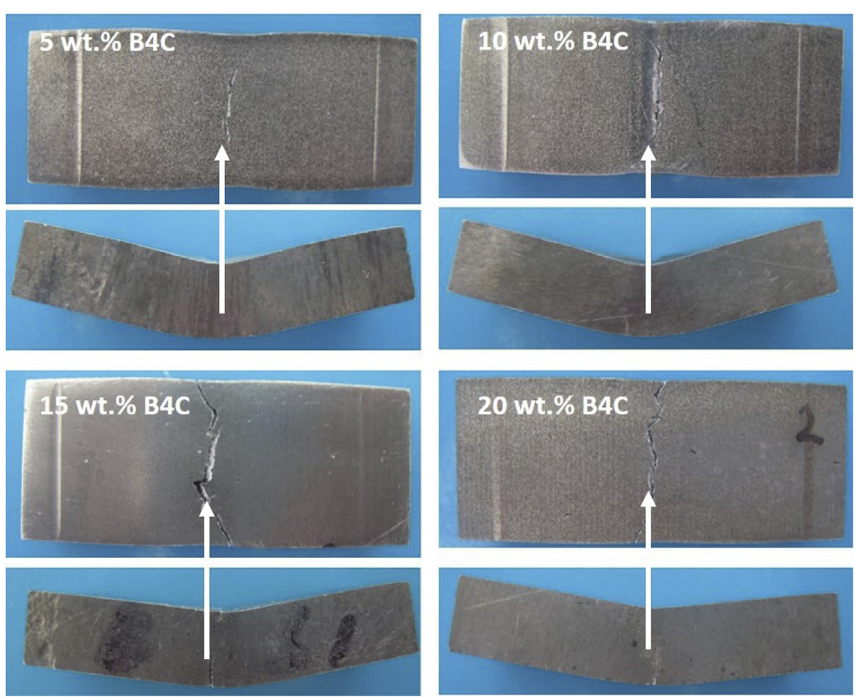

Fig. 5. Photographic views for transverse rupture strength of the composite specimens under study.

$$\mathrm{MSD} = \left(y_1^2 + y_2^2 + y_3^2 + \ldots\ldots\ldots + y_n^2\right) \Big/ n, \tag{1}$$

$$S/N = -10 \times Log_{10}(MSD)\ , \tag{2}$$

where y is the measured surface roughness and n is the number of measurements made.

The experimental results for surface roughness and energy consumption are presented in Table 4. Figs. 7 and 8 show how the milling parameters affect the surface roughness and power consumption for MMCs machined under dry- and compressed-air cooling. The best machining variables and the optimal value for each milling parameter are given in Table 5. The effect of the noise in the experimental system is minimal for the highest S/N; hence, the optimal milling parameters are determined based on the highest S/N for the machining parameters. Based on the response

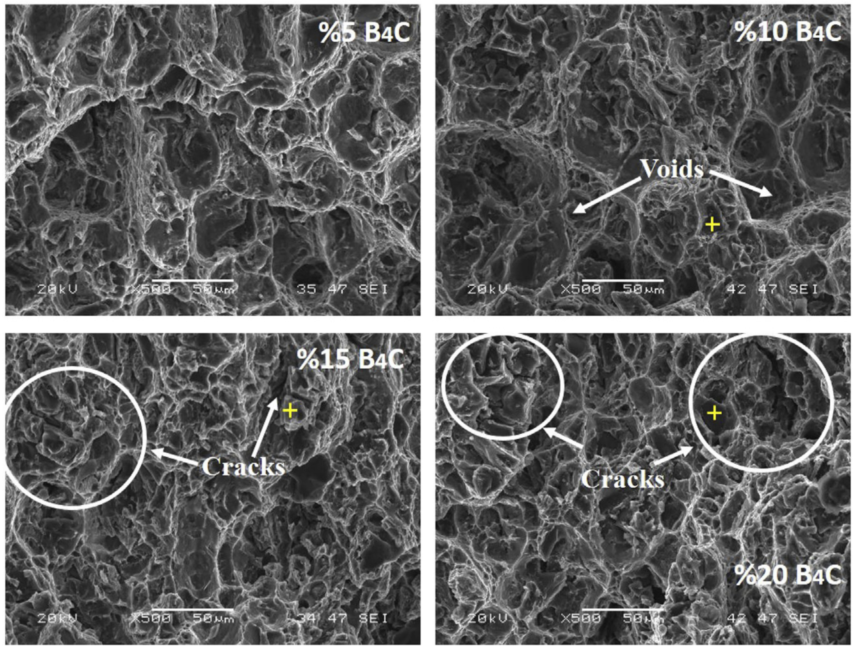

Fig. 6. SEM fractographs for fracture surfaces of composite specimens under study.

table (Table 5) for S/N and the mean effects (Fig. 7), the optimal milling parameters for surface quality is Al6061 alloy reinforced with 15 wt% B_4C (A_3), a milling speed (B_4) of 480 m/min, a cutting feed per tooth (C_1) of 0.08 mm/tooth, and an axial cutting depth (D_1) of 0.8 mm under dry-cutting conditions (E_1). Similarly, based on the criteria of smaller power consumption and higher S/N from the response table (Table 5) and mean effects (Fig. 8), the minimum energy consumption occurs for milling Al6061 alloy reinforced with 10 wt% B_4C (A_2), a milling speed (B_1) of 220 m/min, a cutting feed (C_4) of 0.16 mm/tooth, and an axial depth of cut (D_1) of 0.8 mm under dry-cutting conditions (E_1).

We used analysis of variance (ANOVA) to evaluate the experimental results for surface roughness and energy consumption. Based on the ANOVA results, the cutting feed per tooth is the most effective milling parameter for determining surface roughness with a contribution of 63%, followed by axial cutting depth, milling speed, and cutting environment with contributions of 14%, 9%, and 8%, respectively. Similarly, the milling speed (79%) and axial cutting depth (14%) are the most effective milling parameters for determining power consumption (Table 6). The feed rate and cutting conditions do not strongly affect the energy consumption of the milling machine tool. Increasing milling speed combined with lower cutting feeds results in an improved surface quality but leads to greater power consumption. The quality of the machined surface decreases as the cutting-feed rate increases, whereas power consumption remains almost constant from 0.08 to 0.12 mm/tooth. For the milling of all composite specimens, the surface roughness and power consumption increase with the axial cutting depth. The surface quality decreases for milling of all workpiece materials under compressed-air cooling and energy consumption increases only for 1%. According to the mean-effect plot (Fig. 8), under compressed-air cooling, the energy consumption of the machine

Table 4
Results of measurements, S/N, and surface roughness.

Test no.	Control factors					Surface roughness *Ra* (*μm*)	S/N ratio for *Ra* (dB)	Power *P* (*W*)	S/N ratio for *P* (dB)
	A	B	C	D	E				
	Material (*M*)	Milling speed (*Vc*)	Feed rate (f_z)	Axial depth of cut (a_p)	Cutting environment (*ce*)				
1	1	1	1	1	1	0.274	11.24	160	−44.08
2	1	2	2	2	1	0.294	10.63	300	−49.54
3	1	3	3	3	2	0.323	9.82	500	−53.98
4	1	4	4	4	2	0.346	9.22	690	−56.78
5	2	1	2	3	2	0.311	10.14	225	−47.04
6	2	2	1	4	2	0.309	10.20	420	−52.47
7	2	3	4	1	1	0.320	9.90	300	−49.54
8	2	4	3	2	1	0.291	10.72	525	−54.40
9	3	1	3	4	1	0.325	9.76	300	−49.54
10	3	2	4	3	1	0.326	9.74	270	−48.63
11	3	3	1	2	2	0.287	10.84	485	−53.71
12	3	4	2	1	2	0.270	11.37	550	−54.81
13	4	1	4	2	2	0.344	9.27	225	−47.04
14	4	2	3	1	2	0.308	10.23	300	−49.54
15	4	3	2	4	1	0.296	10.57	580	−55.27
16	4	4	1	3	1	0.263	11.60	675	−56.59

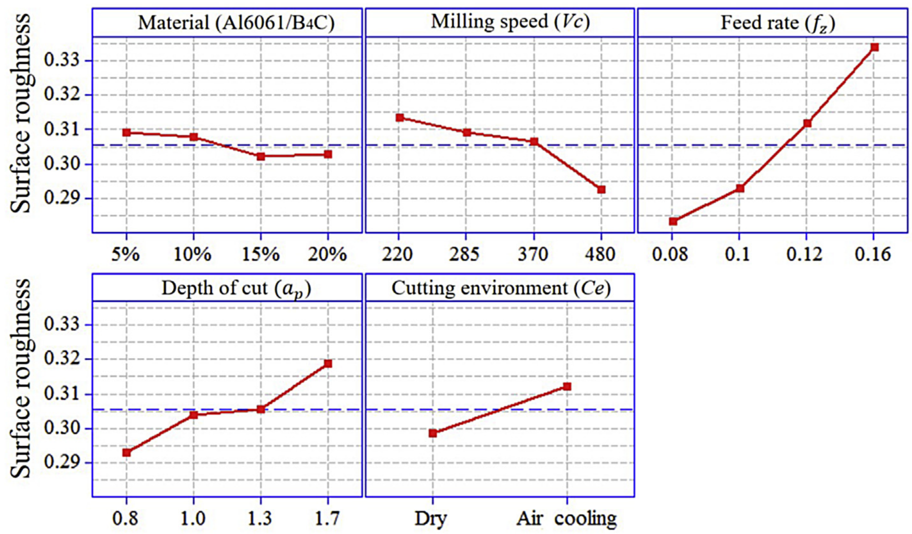

Fig. 7. Mean effects of milling parameters on surface roughness.

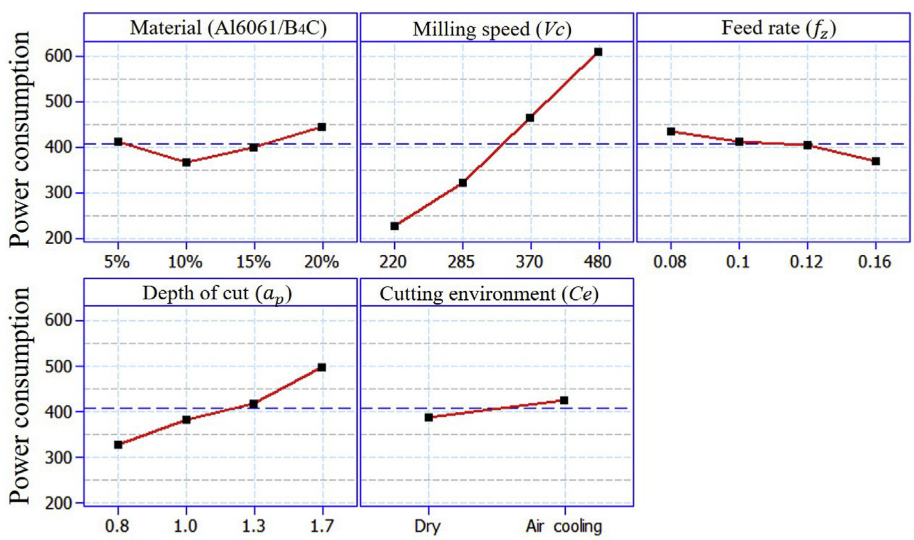

Fig. 8. Mean effects of milling parameters on power consumption.

tool during milling is maximal when the milling speed and depth of cut are greatest for milling Al6061 reinforced with 20 wt% B_4C. Increasing the machining speed reduces the life of the cutting tool more significantly than do the other machining parameters, such as feed rate and depth of cut. Furthermore, the energy required by the machine tool increases with the cutting speed [18]. Under dry-cutting conditions and for milling Al6061 reinforced with 10 wt% B_4C, the minimal energy required by the milling machine occurs when the cutting speed and axial cutting depth are the smallest and the feed rate is the greatest. The energy consumed by the milling machine diminishes because the time required to machine the workpiece decreases at higher feed rates. Based on the experimental results, milling speed is the most significant machining parameter to minimize power consumption; hence, the lowest milling speed should be used to minimize power consumption. The right cutting parameters such as cutting speed, table feed and axial depth of cut for the machining operation is important for the productivity in milling process. In order to maintain better surface quality, lower feed rates may have to be chosen resulting in low productivity. However, the experimental results indicated that it could be possible to minimize the surface quality errors without compromising the productivity at higher cutting depth and cutting

Table 5
Response table for signal to noise ratios for surface roughness, smaller is better.

Level	*M*	V_c	f_z	a_p	*Ce*
Surface roughness Ra					
1	10.228	10.105	10.972	10.686	10.521
2	10.241	10.200	10.681	10.367	10.137
3	10.428	10.282	10.132	10.324	
4	10.418	10.729	9.530	9.939	
Delta	0.200	0.623	1.442	0.747	0.385
Rank	5	3	1	2	4
Power consumption P					
1	−51.10	−46.93	−51.71	−49.49	−50.95
2	−50.86	−50.04	−51.67	−51.18	−51.92
3	−51.67	−53.13	−51.87	−51.56	
4	−52.11	−55.64	−50.50	−53.51	
Delta	1.25	8.72	1.37	4.02	0.97
Rank	4	1	3	2	5

Table 6
Analysis of variance of (a) surface roughness and (b) power consumption.

Source	DF	SeqSS	AdjMS	F	P	Contribution rate (%)
(*a*)						
Regression	5	0.00887	0.0017744	39.438	0.000003	
M	1	0.00013	0.0001275	2.834	0.123191	1
Vc	1	0.00086	0.0008646	19.217	0.001369	9
fz	1	0.00587	0.0058653	130.362	0.000000	63
ap	1	0.00127	0.0012720	28.272	0.000339	14
Ce	1	0.00074	0.0007426	16.504	0.002277	8
Error	10	0.00045	0.0000450			5
Total	15	0.00932				100
(*b*)						
Regression	5	409020	81804	58.786	0.000000	
M	1	3445	3445	2.476	0.146682	1
Vc	1	333465	333465	239.634	0.000000	79
fz	1	7900	7900	5.677	0.038434	2
ap	1	59133	59133	42.494	0.000067	14
Ce	1	5077	5077	3.648	0.085205	1
Error	10	13916	1392			3
Total	15	422936				100

speed [31].

3.3. Machining properties

In this study, all milling experiments were carried out with two passes for all the cutting parameters. The detailed tool wear mechanism was not investigated nevertheless the cutting tool behavior was analyzed utilizing SEM micrographs to understand the outcome of surface quality and power consumption. As shown in Figs. 12 and 13, it was observed that the tool wear was changed with respect to the reinforcement fraction of B_4C and cutting conditions. The cutting insert failure by fracturing was not observed during the experiments and machining was stable. A small quantity of BUE formation was noticed at higher cutting speed and feed rate combination in the milling of 5 wt% B B_4C [Fig. 12(a) and (b), respectively]. For this reason, the quality of machined surface was decreased. Abrasion and cutting tool chipping were observed at higher feed rates in connection with higher B_4C volume of reinforcement particles in the matrix structure. In addition to this, surface quality was not affected adversely at lower feed rates and higher cutting speeds. Fig. 9 (a) shows how the reinforcement fraction and milling speed interact to affect surface quality. At low cutting speed (220 m/min), the alloy reinforced with 5 wt% B_4C has a better surface quality compared with the other composite materials. However, the surface roughness increases approximately linearly with cutting speeds for Al6061 with 5 wt% B_4C. This result is attributed to the creation of a BUE formation on the cutting surface of the insert and the soft structure of the 5 wt% B_4C composite material [Fig. 12 (a) and (b)]. Increasing the fraction of B_4C has a positive effect on the roughness and the finished surface improves upon increasing the milling speed due to the decreasing friction and BUE creation on the tool surface, as noted in previous studies [26,32]. This result could also be due to a decrease in the coefficient of friction between the workpiece material and the cutting tool that occurs due to the increasing flow of the workpiece material. In all machining cases, the surface quality deteriorates upon increasing the cutting feed as can be seen in Fig. 10. This result is expected and is consistent with results from previous studies because the maximum chip thickness increases at higher feed rates, which results in an increase in cutting forces and thereby a decrease in surface quality [20,21]. For dry cutting, the best surface roughness occurs at the greatest milling speed and the lowest feed rate.

We examine the SEM micrographs of the machined surface of composite specimens to specify the quality of the finished surface. To investigate the existence of surface detriments in the form of tiny holes, cracks, and smeared material, finished surfaces of experimental MMCs are also analyzed using an optical microscope at various magnifications. The optical micrographs are presented in

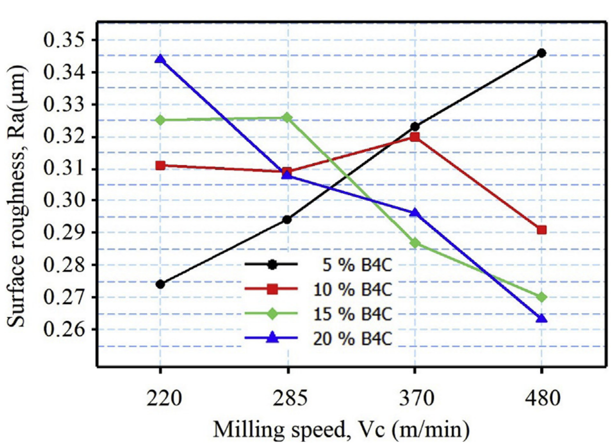

Fig. 9. Surface roughness as a function of milling speed and composite material on *Ra*.

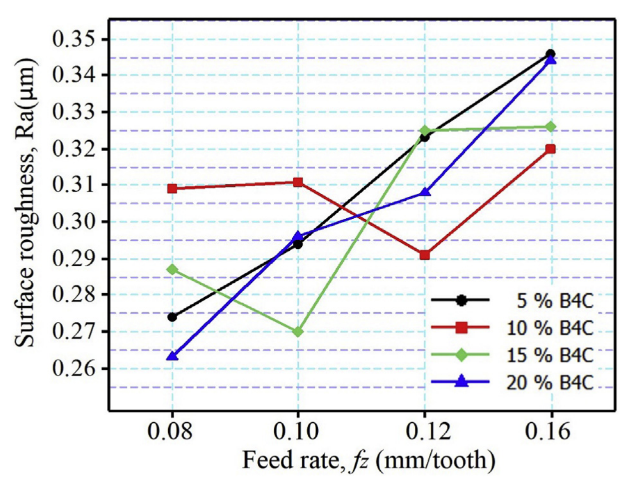

Fig. 10. Surface roughness as a function of cutting-feed rate.

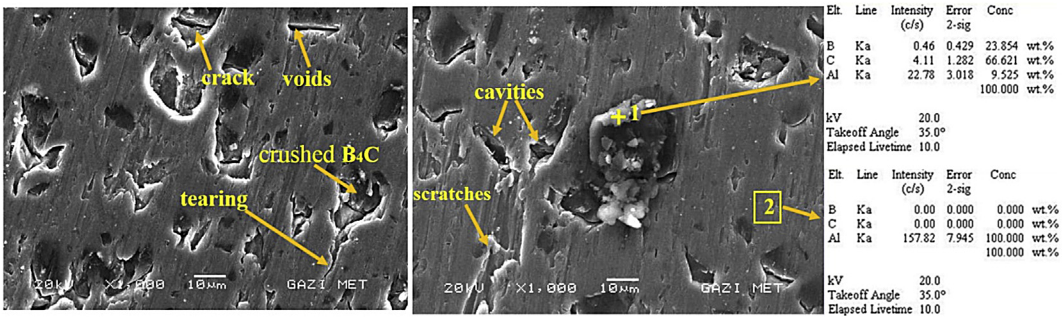

Fig. 11. SEM micrograph of machined surface of Al6061/10 wt% B_4C at high magnification.

Fig. 2, and SEM micrographs of machined composite materials are shown in Fig. 3. The SEM micrographs reveal short and long scratches parallel to the direction of the machining for the machined surface of Al6061 reinforced with 5 wt% B_4C. This result may be attributed to BUE creation on the cutting tool because of the soft structure of this composite material and the machining parameters. Al6061 reinforced with 5 wt% B_4C is softened at higher milling speeds, which can increase the adhered aluminum material on cutting tool. Small quantities of melted aluminum alloy are noticeable on the cutting tool in the milling of 10 wt% B_4C and 15 wt % B_4C [Fig. 12(a) and (b), respectively]. This formation causes small surface scratches because of the friction between workpiece and cutting tool. During milling, some B_4C particles are partially pulled out of the matrix structure, leaving behind tiny holes in the machined surface. Fig. 11 shows a SEM micrograph of a machined surface of a composite sample at high magnification, with several small cavities and crushed B_4C particles labeled. The interfacial bonding between aluminum alloy and B_4C particles also affects the machinability of MMCs. Some B_4C particles in the aluminum matrix are totally detached from the matrix because of the weak interfacial bond, leading to voids and making a clear contour around the B_4C particles. Some B_4C particles are removed from the matrix structure and are dragged under the cutting tool along the machined surface for a short distance, thereby damaging the surface (see Fig. 11).

Fig. 13 shows that some tool breakage occurred on the cutting insert during milling of 20 wt% B_4C at a cutting speed of 480 m/min, a feed rate of 0.16 mm/tooth, and an axial cutting depth of 1 mm under dry-cutting conditions. However, the surface quality improves upon increasing the reinforcement fraction. This result is attributed to the lack of BUE created on the cutting tool, which depends on the machining parameters when milling B_4C-reinforced composites [26,32]. To summarize, excellent surface roughness and acceptable cutting performance from the cutting insert at lower cutting speeds are obtained for milling of all workpiece materials. Acceptable milling performance of the cutting insert at lower milling speeds might be due to BUE formation,

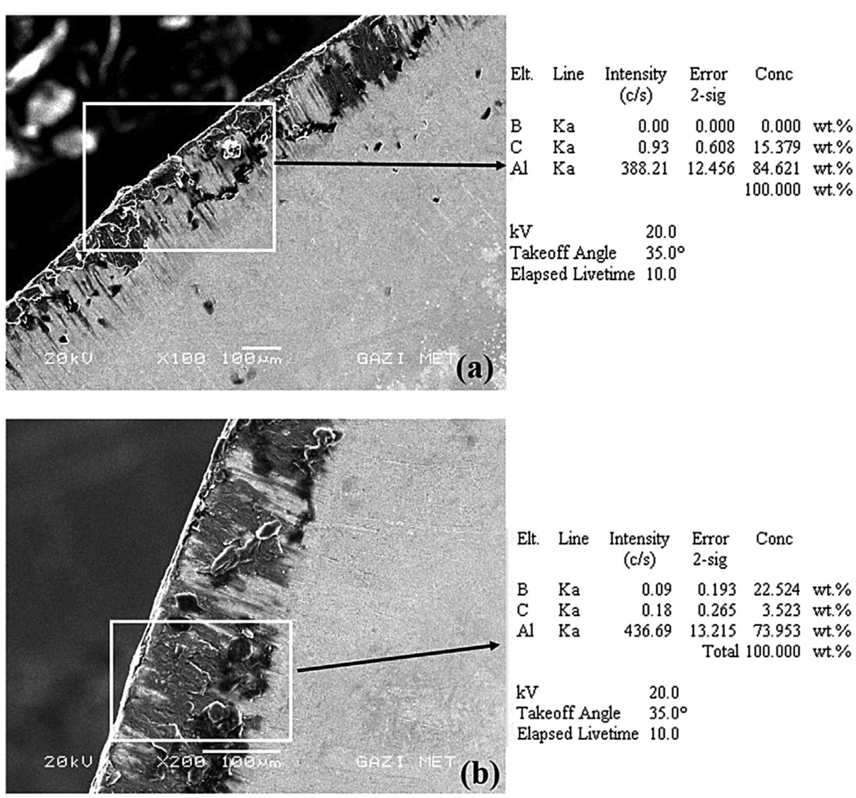

Fig. 12. SEM micrographs of cutting insert after machining process (a) at cutting speed of 480 m/min and (b) at cutting speed of 370 m/min in milling of 5 wt% B_4C.

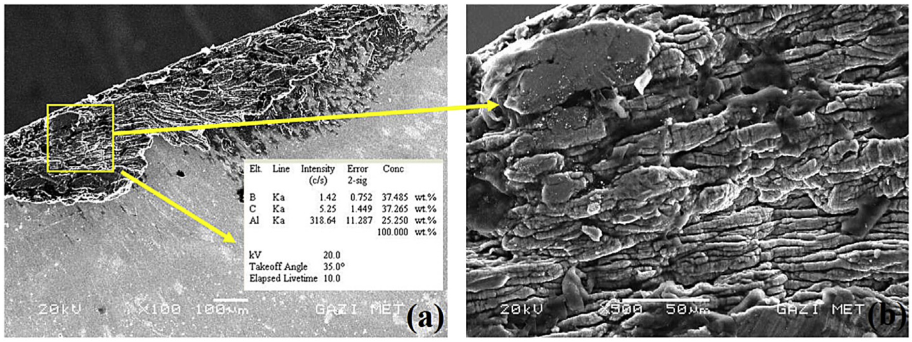

Fig. 13. SEM micrographs of cutting insert after milling process at cutting speed of 480 m/min in milling of 20 wt% B_4C.

which forms a thin film between the tool and workpiece to protect the tool surface.

4. Conclusions

In this study, Al6061 reinforced with 5–20 wt% B_4C was produced using a powder metallurgy method. Hardness, fracture toughness, tensile and transverse rupture strengths of the composite specimens were investigated. The influence of B_4C particles on surface roughness and energy consumption was studied as a function of milling parameters under dry- and compressed-air cooling and with an uncoated carbide insert. The main findings of this study are the following:

- The optical and SEM micrographs show that B_4C particles are homogeneously distributed in all composite specimens and achieved good interfacial bonding with the matrix.
- The fracture toughness, hardness, transverse rupture strength and tensile strength were affected by the weight fraction of B_4C reinforcement content used in the matrix. The hardness of composite specimens increases with B_4C content and the maximum hardness occurs for 20 wt% B_4C. The impact resistance decreases with increasing fraction of B_4C reinforcement in the matrix and the maximum fracture toughness occurs for 10 wt% B_4C. The highest tensile and transverse rupture strengths are for Al6061/5 wt% B_4C.
- Desirable surface roughness is found for milling of all composites materials and the surface quality improves with B_4C content while increasing mechanical properties of MMCs. The best surface roughness occurs at high milling speed, and the lowest feed rate under dry-cutting conditions and the best surface quality occurs for milling Al6061 alloy reinforced with 15 wt% B_4C.
- For surface quality in terms of the productivity, the optimal machining conditions are for milling Al6061 alloy reinforced with 15 wt% B_4C, machining speed at 480 m/min, feed rate at 0.08 mm/tooth, and axial cutting depth at 0.8 mm under dry-cutting conditions.
- The lowest power consumption is for milling Al6061 alloy reinforced with 10 wt% B_4C, milling speed at 220 m/min, cutting feed at 0.16 mm/tooth, and axial depth of cut at 0.8 mm under dry-cutting conditions.
- For surface quality, the most influential milling parameter was cutting feed, with a contribution of 63%. The axial depth of cut, cutting speed, and cutting conditions contribute 14%, 9%, and 8%, respectively. Thus, the surface quality is better at lower feed rate.
- For energy consumption, cutting speed is the most significant machining parameter, with a contribution of 79%. The lowest milling speed must be used to achieve minimal power consumption under dry-cutting conditions.
- Surface roughness and energy consumption increase during milling of all composite workpiece materials when machining under compressed-air cooling.
- For milling the composites, the cutting insert indicated performed acceptably at low milling speeds and feed rates.

The experimental findings are expected to provide useful guidelines for the efficient planning of the machining parameters in terms of improved productivity, workpiece quality and reduced production cost.

Acknowledgments

The authors wish to thank Hacettepe University Scientific Research Projects Coordination Unit for the financial support through project number #014 D05 603 001-636. The authors would like also to thank Poyraz CNC for cutting the specimens. Special thanks go to ASO technical college and Muzaffer Hasbal for executing the milling experiments.

References

[1] Thuault A, Marinel S, Savary E, Heuguet R, Saunier S, Goeuriot D, et al. Processing of reaction-bonded B_4C–SiC composites in a single-mode microwave cavity. Ceram Int 2013;39:1215–9.
[2] Domnich V, Reynaud S, Haber RA, Chhowalla M. Boron carbide: structure, properties, and stability under stress. J Am Ceram Soc 2011;94:3605–28.
[3] Shin YC, Dandekar C. Machining of metal matrix composites. 2012.
[4] Wang J, Lin W, Jiang Z, Duan L, Yang G. The preparation and properties of SiCw/B_4C composites infiltrated with molten silicon. Ceram Int 2014;40:6793–8.
[5] Manna A, Bhattacharayya B. A study on machinability of Al/SiC-MMC. J Mater Process Technol 2003;140:711–6.
[6] Soy U, Ficici F, Demir A. Evaluation of the Taguchi method for wear behavior of Al/SiC/B_4C composites. J Compos Mater 2011;46:851–9.
[7] El-Gallab M, Sklad M. Machining of Al/SiC particulate metal-matrix composites Part I: tool performance. J Mater Process Technol 1998;83:151–8.
[8] Rajkumar K, Charles JMA, Kumar KV, Praveen JJC, Padmanathan A. In: Proceedings of the national conference on emerging trends in mechanical engineering; 2013. p. 306–12.
[9] Ibrahim MF, Ammar HR, Samuel AM, Soliman MS, Almajid A, Samuel FH. Mechanical properties and fracture of Al–15 vol.-% B_4C based metal matrix composites. Int J Cast Met Res 2014;27:7–14.
[10] Ibrahim MF, Ammar HR, Samuel AM, Soliman MS, Samuel FH. On the impact toughness of Al-15 vol.% B_4C metal matrix composites. Compos Part B 2015;79:83–94.
[11] Baradeswaran A, Perumal AE. Influence of B_4C on the tribological and mechanical properties of Al 7075– B_4C composites. Compos Part B 2013;54:146–52.
[12] Karabulut Ş, Gökmen U, Çinici H. Study on the mechanical and drilling properties of AA7039 composites reinforced with Al_2O_3/B_4C/SiC particles. Compos Part B 2016;93:43–55.
[13] Joshua OS, David MO, Sikiru IO. Experimental investigation of cutting parameters on surface roughness prediction during end milling of aluminium 6061 under MQL. Mech Eng Auto 2015;5:1–13.
[14] Lou MS, Chen JC, Li CM. Surface roughness prediction technique for CNC end-milling. J Ind Technol 1998;15:1–6.

[15] Lillo TM. Enhancing ductility of Al6061+10wt% B_4C through equal-channel angular extrusion processing. Mater Sci Eng A 2005;410:443–6.
[16] Chen LJ, Ma CY, Stoica GM, Liaw PK, Xu C, Langdon TG. Mechanical behavior of a 6061 Al alloy and an Al_2O_3/6061 Al composite after equal-channel angular processing. Mater Sci Eng A 2005;410:472–5.
[17] Rao PN, Singh D, Brokmeier HG, Jayaganthan R. Effect of ageing on tensile behaviour of ultrafine grained Al 6061 alloy. Mater Sci Eng A 2015;641:391–401.
[18] Camposeco-Negrete C. Optimization of cutting parameters using Response Surface Method for minimizing energy consumption and maximizing cutting quality in turning of AISI 6061 T6 aluminum. J Clean Prod 2015;91:109–17.
[19] Patel PR, Patel VA. Effect of machining parameters on surface roughness and power consumption for 6063 Al alloy TiC composites (MMCs). Int J Eng Res Appl (IJERA) 2012;2(4):295–300.
[20] Muñoz-Escalona P, Shokrani A, Newman ST. Influence of cutting environments on surface integrity and power consumption of austenitic stainless steel. Rob Comput Integr Manuf 2015;36:60–9.
[21] Smith WF. Structure and properties of engineering alloys. second ed. New York: McGraw-Hill; 1993.
[22] Swamy ARK, Ramesha A, Kumar GV, Prakash JN. Effect of particulate reinforcements on the mechanical properties of Al6061-WC and Al6061-Gr MMCs. J Min Mater Charac Eng 2011;10:1141.
[23] Metal powder industries federation: standard test methods for metal powders and powder metallurgy products, New jersey. 1998.
[24] Metal powder industries federation: standard test methods for metal powders and powder metallurgy products, Newjersey. 1998.
[25] ISO 8688–1 Tool life testing in milling. Part 1: face milling. International ISO Standard; 1989.
[26] Karabulut Ş. Optimization of surface roughness and cutting force during AA7039/Al_2O_3 metal matrix composites milling using neural networks and Taguchi method. Measurement 2015;66:139–49.
[27] Sahoo AK, Pradhan S. Modeling and optimization of Al/SiCp MMC machining using Taguchi approach. Measurement 2013;46:306–7.
[28] Geometrical Product Specifications (GPS). Surface texture: profile method, terms, definitions and surface texture parameters. International Organization for Standardization; 1997. ISO-4287.
[29] Chen HS, Wang WX, Li YL, Zhang P, Nie HH, Wu QC. The design, microstructure and tensile properties of B_4C particulate reinforced 6061Al neutron absorber composites. J Alloys Compd 2015;632:23–9.
[30] Roy RK. A primer on the Taguchi method. Society of Manufacturing Engineers; 1990.
[31] Budak E. Analytical models for high performance milling. Part I: cutting forces, structural deformations and tolerance integrity. Int J Mach Tools Manuf 2006;46(12):1478–88.
[32] Reddy NSK, Kwang-Sup S, Yang M. Experimental study of surface integrity during end milling of Al/SiC particulate metal–matrix composites. J Mater Process Technol 2008;201(1):574–9.